THE JOURNAL OF PHYSICAL CHEMISTRY Letters

Perspective

pubs.acs.org/JPCL

Exploring the Dynamics of the Photoinduced Ring-Opening of Heterocyclic Molecules

Michael N. R. Ashfold,* Matthew Bain, Christopher S. Hansen, Rebecca A. Ingle, Tolga N. V. Karsili,† Barbara Marchetti,‡ and Daniel Murdock§

School of Chemistry, University of Bristol, Bristol, United Kingdom, BS8 1TS

Supporting Information

ABSTRACT: Excited states formed by electron promotion to an antibonding σ^* orbital are now recognized as key to understanding the photofragmentation dynamics of a broad range of heteroatom containing small molecules: alcohols, thiols, amines, and many of their aromatic analogues. Such excited states may be populated by direct photoexcitation, or indirectly by nonadiabatic transfer of population from some other optically excited state (e.g., a $\pi\pi^*$ state). This Perspective explores the extent to which the fast-growing literature pertaining to such $(n/\pi)\sigma^*$-state mediated bond fissions can inform and enhance our mechanistic understanding of photoinduced ring-opening in heterocyclic molecules.

All but a few very small molecules absorb near-ultraviolet (UV) photons. Absorption results in formation of electronically excited molecules, which can display a diverse range of photophysical behaviors. Some molecules are remarkably photostable, and return to their ground state by fluorescing. Dye molecules (fluorophores) such as those used in dye lasers, in single molecule spectroscopy, and in super-resolution imaging constitute obvious examples.[1−5] Other molecules like the DNA bases[6] or commercial sunscreen ingredients like avobenzene, oxybenzone, or many cinnamate derivatives[7] have extremely short-lived excited states, show no fluorescence, and yet are also deemed photostable. In these cases, the excited state molecules find efficient nonradiative decay paths back to the ground state. Such nonradiative decay depends on nuclear distortions that bring the potential energy surfaces (PESs) for the excited and ground electronic states of the molecule into near degeneracy, i.e., so-called regions of conical intersection (CI) between the PESs.[8−12] Examples of nuclear motions that enable excited state population to funnel through such CIs include intramolecular proton transfers (e.g., *keto-* ↔ *enol*-isomerism), *cis-* ↔ *trans*-isomerism, and, in the case of cyclic molecules, out-of-plane ring distortions. Photostability in these cases requires that (i) the excited state PES has an appropriate topography, specifically that there is no significant energy barrier between the geometry at which the photoexcited molecule is prepared and that of the CI, and (ii) the nuclear distortions driving the internal conversion (IC) process are eventually "corrected" after crossing to the ground state PES, thereby ensuring that the molecule suffers no net change as a result of the 'excitation−recovery' cycle.[7]

Photodamage—wherein the starting molecule is effectively transformed or destroyed—is another limiting fate of UV photon absorption. Photoinduced bond fission (i.e., photodissociation) is a common example of such a process, and is the theme of this Perspective. Many recent studies have recognized the key roles of $(n/\pi)\sigma^*$ states in enabling excited state bond fissions.[13] These are states formed by promoting an electron from a lone pair (n) or bonding (π) molecular orbital to an antibonding σ^* orbital, which, from here on, will often simply be generically labeled as $\pi\sigma^*$. One further aspect of book keeping: throughout, labels like $^1\pi\sigma^*$ will be reserved for diabatic states, and S_0, S_1, S_2, etc. are used when referring to the adiabatic singlet states.

The lead players (molecules) in this Perspective—dimethylsulfide (MeSMe), thioanisole (PhSMe), thiophene, and various thiophene derivatives—are shown in Figure 1. The Perspective starts by summarizing aspects of the near UV photochemistry of MeSMe and PhSMe in the gas phase. Both molecules contain a C−S−C linkage and undergo $^1\pi\sigma^*$-state-mediated S−C bond fission. Thioanisole (and thiophenols) have been featured in recent studies aimed at determining the extent to which dynamical insights from gas phase studies can inform our knowledge and understanding of the early time dynamics induced by UV photoexcitation of the corresponding molecules in solution. The parallels revealed by such comparative studies, in turn, encourage the use of solution-phase samples and ultrafast pump−probe transient absorption (TA) methods to demonstrate $^1\pi\sigma^*$-state-mediated S−C bond extension and fission in heterocycles like 2(5H)-thiophenone (2-thiophenone from hereon)—a simple five-membered heterocyclic α-carbonyl compound that

Received: May 16, 2017
Accepted: June 29, 2017
Published: June 29, 2017

DOI: 10.1021/acs.jpclett.7b01219
J. Phys. Chem. Lett. 2017, 8, 3440−3451

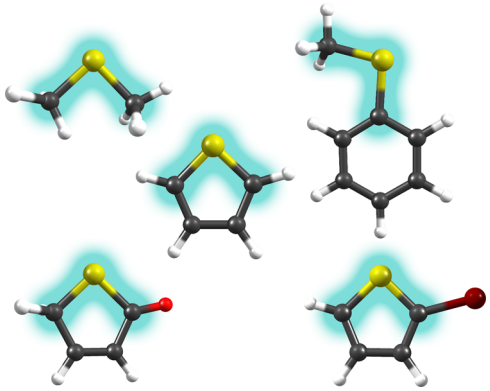

Figure 1. Equilibrium structures of dimethylsulfide, thioanisole, thiophene, 2-thiophenone, and 2-bromothiophene, highlighting the C−S−C motif common to all five species, with S, C, O and Br atoms represented in yellow, black, red, and purple, respectively.

also contains a C−S−C linkage. We conclude by returning to the gas phase and surveying recent progress in exploring dynamical aspects of the photoinduced ring-opening of other thiophene derivatives and, then, of other cyclic molecules.

Gas Phase Photochemistry of MeSMe and PhSMe. Figure 2 shows cuts through the PESs for the ground and first few excited singlet states of MeSMe, PhSMe, and thiophene, along one S−C bond. The PECs for extending an S−Me bond (R_{S-Me}) in dimethylsulfide shown by red lines in Figure 2a apply for the ground state equilibrium geometry (∠CSC ~ 99°). The ground state of MeSMe has $^1A'$ symmetry (in C_s) and, at this bent geometry, its PEC correlates with ground ($\tilde{X}$)-state Me and MeS radical products. The first excited state, a dissociative state of $^1A''$ symmetry formed by excitation from the highest occupied molecular orbital (HOMO), the S($3p_x(a'')$) orbital, to a $\sigma^*(a')$ orbital localized along one S−Me bond, correlates to this same limit. This is one of two near-degenerate states of $^1A''$ symmetry reached by vertical excitation from the ground state minimum energy geometry (the other state has substantial Rydberg character). The diabatic PECs for these two $^1A''$ states exhibit a conical intersection at small R_{S-Me} (labeled CI-1 in Figure 2a), and the interaction of these two $^1A''$ states is revealed by the diffuse resonance structure apparent in the parent absorption spectrum.[14,15] Figure 2a shows one higher energy PEC as a red line. This is for a dissociative $^1\pi\sigma^*$ state of $^1A'$ symmetry that, at bent geometries, correlates to ground-state Me($\tilde{X}$) plus electronically excited ($\tilde{A}$ state) MeS products. The starting orbital in this case is an in-plane ~$sp^2(a')$ orbital on the S atom.

Note, these PECs are just what is implied by the acronym: one-dimensional cuts through multidimensional PESs, which may—and in this case do—have very different topographies in other coordinates. This is illustrated by the black lines in Figure 2a, which show the corresponding potentials when ∠CSC = 180°. In this higher symmetry (linear) limit, the ground state of MeSMe has the term symbol $^1\Sigma$, and its PEC correlates diabatically with Me($\tilde{X}$) + MeS($\tilde{A}$) products. The S atom in the MeS radical supports five nonbonding electrons, distributed between two p (π) orbitals and an on-axis sp-hybrid (σ) orbital. Viewed in this way, the $\tilde{X}$ and $\tilde{A}$ states of the MeS radical have respective configurations $\pi^3\sigma^2$ and $\pi^4\sigma^1$ and, as Figure 2a shows, the collinear approach of ground state Me and MeS radicals results in a repulsive interaction. This is the long-range part of a $^1\Pi$ excited state of (linear) MeSMe formed by

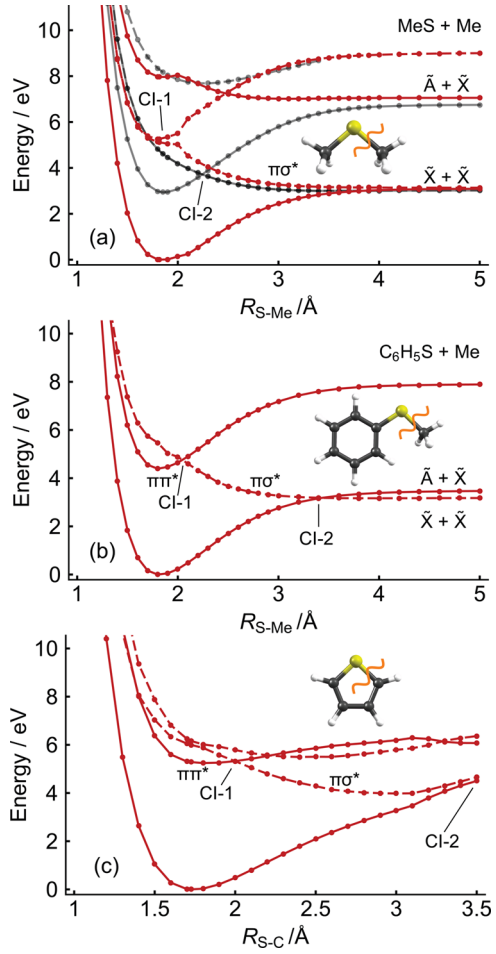

Figure 2. Calculated PECs along the S−C bond highlighted in the accompanying structure for the ground and first few singlet excited states of (a) MeSMe, at its equilibrium bent geometry (red lines) and at ∠CSC = 180° (black lines), (b) PhSMe, and (c) thiophene—both at planar geometries. Solid and dashed lines are used to distinguish states of A' and A'' symmetry, respectively, and conical intersections CI-1 and CI-2 are indicated in each case. Further details are provided in the Supporting Information.

$\sigma^* \leftarrow \pi$(HOMO) promotion, which splits into the dissociative $^1A''$ and $^1A'$ states on bending the C−S−C frame. As Figure 2a also shows, the former potential is (relatively) unaffected by such bending, whereas the latter forms a conical intersection (CI-2 in Figure 2a) with the ground state PES. Interested readers are referred to ref 13 for more examples of the importance of such $\pi\sigma^*$ states in the excited state photochemistry of numerous molecular prototypes.

S−Me bond fission following near-UV photoexcitation of jet-cooled MeSMe has been investigated by velocity map imaging (VMI) methods.[15,16] Figure 3a,b shows images of the Me and MeS fragments formed by photoexcitation of jet-cooled MeSMe molecules at 227.5 nm and detected using "universal" (118 nm) photoionization. Both images are annular, confirming that the fragments are formed translationally excited. The radial distribution in each image allows determination of the respective fragment recoil velocities, confirms that the two sets of products are momentum matched, and allows calculation of the total kinetic energy of the Me + SMe products. Energy conservation considerations confirm that both fragments are formed in their electronic ground states. The

DOI: 10.1021/acs.jpclett.7b01219
J. Phys. Chem. Lett. 2017, 8, 3440−3451

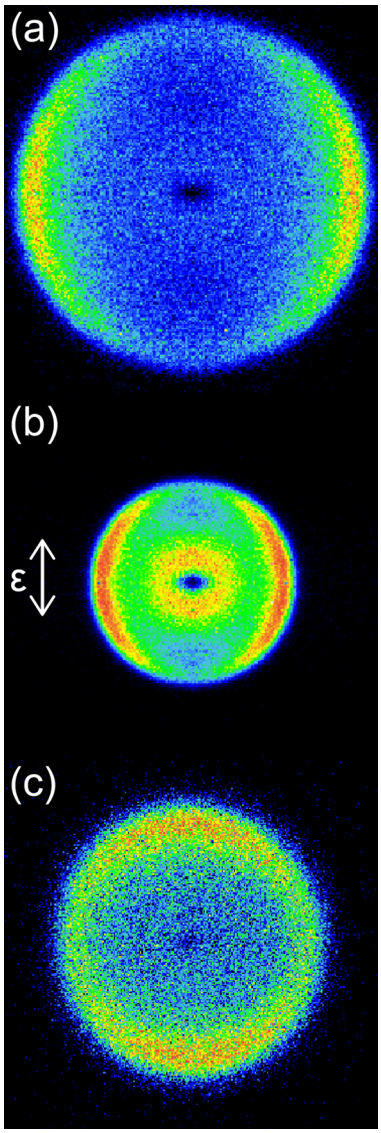

Figure 3. Images of the (a) Me (all v) and (b) MeS (all v) fragments formed by photolysis of jet-cooled MeSMe at 227.5 nm and ionised by 118 nm single photon ionization, and (c) Me (v = 0) fragments formed by photolysis of jet-cooled PhSMe at 289.8 nm and detected by 2 + 1 REMPI at 333.6 nm. The inner annulus in image b is the (unwanted) 118 nm-laser-only signal. The electric vector of the photolysis laser radiation in all cases was vertical, in the plane of the detector, as shown by the double headed arrow in image b.

(comparative) narrowness of the annuli shows that both fragments are formed in a limited spread of internal (vibrational, rotational) energy states. Comparison with previously reported images obtained using resonance-enhanced multiphoton ionization (REMPI) methods[15,16] confirms that most of the Me fragments are formed in their zero-point (v = 0) vibrational level. The image is also anisotropic, revealing an angular distribution consistent with prompt fission of one S−Me bond following $\sigma^*(a') \leftarrow 3p_x(a'')$ excitation, the transition dipole moment for which lies perpendicular to the molecular plane. These findings are fully consistent with dissociation on the $^1\pi\sigma^*(^1A'')$ PES.

Now consider S−Me bond fission following near UV excitation of thioanisole, the equilibrium geometry of which has all the heavy atoms in a plane, with ∠CSC ∼ 104°. In this high symmetry limit, the ground state PEC correlates diabatically with a Me radical and electronically excited PhS(Ã) products (Figure 2b). In contrast to MeS, the $3p_x$ and $3p_y$ orbitals of the S atom in the PhS radical are not degenerate, as the $3p_x$ orbital conjugates with the π-system of the ring. The parent → product correlations in this case can be derived by focusing on just three electrons in these S $3p_x(a'')$ and $3p_y(a')$ orbitals of the radical. The X̃ and Ã states of PhS can be represented by the respective configurations $(a')^2(a'')^1$ and $(a')^1(a'')^2$. The in-plane approach of ground-state PhS and Me radicals results in a repulsive interaction which, again, can be attributed to the long-range part of the diabatic $^1\pi\sigma^*$ PEC. The ground and $^1\pi\sigma^*$ PECs again exhibit a conical intersection (CI-2 in Figure 2b) at extended R_{S-Me}. Figure 2b also shows that the lowest singlet state of PhSMe reached by photoexcitation is actually the first $^1\pi\pi^*$ state, the PEC for which shows a conical intersection (CI-1) with the $^1\pi\sigma^*$ state at small R_{S-Me}. Both CIs become regions of avoided crossing as the molecule distorts from planar.

Several VMI studies of the Me(v = 0) fragments resulting from near UV photoexcitation of thioanisole and substituted thioanisoles have been reported,[17−20] and full-dimensional PESs and state-couplings for the three states of PhSMe featured in Figure 2b are also available.[21] Focusing specifically on bare PhSMe, molecules in the $^1\pi\pi^*$(v = 0) level decay so slowly (nsec time scale) that the parent absorption spectrum shows resolved rovibronic structure.[22] Nonetheless, molecules in this level do predissociate. Me radicals are formed and, as Figure 3c shows, these can be imaged. The Me(v = 0) fragments are formed translationally excited with, in this case, a near-isotropic recoil velocity distribution (consistent with the long excited state lifetime). Again, the relative narrowness of the annular ring indicates that the partner PhS fragments are formed in a fairly narrow spread of internal energy states; more detailed analysis reveals that >90% of them are formed in the excited (Ã) electronic state.[17,20]

Viewed from the perspective of PhSMe molecules in the $^1\pi\pi^*(v = 0)$ level, CI-1 presents an energy barrier.

These observations are all consistent with the dissociation dynamics implied by the PECs shown in Figure 2b. Population excited to the $^1\pi\pi^*$ state first has to transfer to the $^1\pi\sigma^*$ continuum by nonradiative coupling in the region of CI-1. Viewed from the perspective of PhSMe molecules in the $^1\pi\pi^*(v = 0)$ level, CI-1 presents an energy barrier. The magnitude of this barrier is reduced if the molecule distorts from planarity, but the barrier still represents an impediment to dissociation and accounts for the observed (long) excited state lifetime. The dissociating molecules thus access the $^1\pi\sigma^*$ PES with nonplanar geometries, and move toward the local minimum associated with CI-2, where their ultimate fate is determined. Any molecules that approach CI-2 with (near) planar geometries are optimally poised for nonadiabatic coupling to the ground state PES and eventual dissociation to Me + PhS(X̃) products. However, the VMI data implies that most dissociating molecules sample the region of CI-2 without recovering planarity, remain on the excited state PES, and dissociate to Me + PhS(Ã) products.[17,20]

DOI: 10.1021/acs.jpclett.7b01219
J. Phys. Chem. Lett. 2017, 8, 3440−3451

The simple few-electron picture used to rationalize CI-2 and the electronic branching in the radicals formed upon S−Me bond fission in PhSMe can be extended to show how analogous photoinduced S−C bond extension in S-containing heterocycles can promote nonadiabatic population transfer (i.e., internal conversion) to the S_0 PES and, potentially, result in ring-opening. To this end, Figure 4a shows the occupancy of key orbitals in the ground and $^1\pi\sigma^*$ excited states of PhSMe, and in the Me + PhS($\tilde{X}/\tilde{A}$) products. The key occupied orbitals in PhSMe(S_0) are taken as the nonbonding S $3p_x(a'')$ orbital and the $\sigma_{S-Me}(a')$ orbital localized on the bond that is destined to break. In this representation, the ground state parent molecule has configuration $(a')^2(a'')^2$, the dissociative $^1\pi\sigma^*$ state is described as $(a')^2(a'')^1(\sigma_{S-Me}{}^*, a')^1$, the $\tilde{X}$ and $\tilde{A}$ states of the PhS radical have respective configurations $(a')^2(a'')^1$ and $(a')^1(a'')^2$, and the parent → product correlations for planar geometries are as shown in Figure 2b.

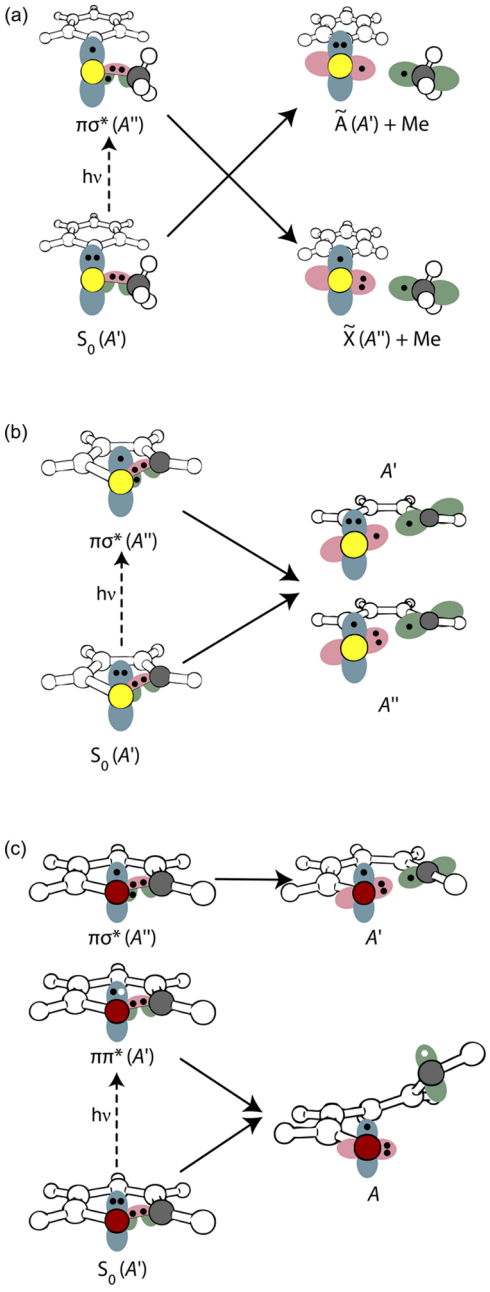

Figure 4. Diagram highlighting the evolving occupancy of key orbitals following near UV photoexcitation leading to (a) S−Me bond fission in PhSMe, (b) S−C bond extension in thiophene, and (c) O−C(O) bond extension in α-pyrone. The key orbitals are the S($3p_x$) orbital in iamges a and b and the $2p_x$ orbital of the O atom in the ring in image c, all shown in blue, and the σ (pink) and σ^* (green) orbitals localized around the extending bond. Electron density in the π^* orbital of α-pyrone is indicated using a white dot in the O($2p_x$) orbital. S, O, and C atoms are depicted in yellow, red, and gray, respectively. For clarity, only atoms associated with the breaking bond are colored.

Figure 2c shows analogous PECs for (planar) thiophene, with the key σ and σ^* (a') orbitals centered on one S−C bond. As Figure 4b shows, photoinduced rupture of this bond following population of the $^1\pi\sigma^*$ state would, in a diabatic picture, result in a biradical with a'' symmetry, and we can anticipate a conical intersection between this and the S_0 PES upon extending one S−C bond. Again, this is labeled CI-2, since the long wavelength UV absorption of thiophene involves $\pi^* \leftarrow \pi$ excitation and the resulting $^1\pi\pi^*$ state population can access the $^1\pi\sigma^*$ state via a CI between the $^1\pi\pi^*$ and $^1\pi\sigma^*$ PESs (CI-1) at shorter R_{S-C} bond lengths, as shown in Figure 2c. Support for this predicted ring-opening following UV photoexcitation of thiophene and nonadiabatic coupling to the ground state PES at CI-2 is provided by more rigorous electronic structure calculations[23−25] and (indirectly) by the results of photofragment translational spectroscopy (PTS) experiments employing universal (synchrotron) vacuum UV (VUV) photoionization detection following 193 nm photoexcitation,[26] and by both time-resolved photoelectron[27] and resonance Raman[28] spectroscopy studies.

> Recent ultrafast UV pump, broadband TA probe studies in solution offer some of the most direct evidence for the formation of ring-opened products following UV excitation of such heterocycles.

Photochemistry of PhSH and PhSMe in Solution. Recent ultrafast UV pump, broadband TA probe studies in solution offer some of the most direct evidence for the formation of ring-opened products following UV excitation of such heterocycles. Before presenting data from such studies, however, it is necessary to consider the extent to which photophysical insights derived from gas phase studies can usefully inform our understanding of the corresponding system in solution, and vice versa, since the transferability between these very different environments is not immediately obvious. The photodissociation of an isolated gas-phase molecule can be viewed as a closed problem: energy and momentum are conserved, and any bond fission is irreversible. The same is not true in the solution-phase. The proximal solvent molecules may modify the PESs relative to those of the isolated solute molecule. Interaction with solvent molecules may dissipate some of the photoexcitation energy prior to bond fission, and will dissipate any excess energy partitioned into the dissociation products. Products that have no analogue in the corresponding gas-phase study may also arise by, for example, geminate recombination.

Nonetheless, there is growing literature showing that gas phase studies can provide a useful guide to the early time photofragmentation dynamics of the corresponding solute

DOI: 10.1021/acs.jpclett.7b01219
J. Phys. Chem. Lett. 2017, 8, 3440−3451

molecule in a weakly interacting solvent. Thiophenols have proven popular test-systems. For example, the H atoms formed in the near UV photolysis of gas-phase 4-methylthiophenol (4-MePhSH) molecules display an anisotropic, bimodal velocity distribution. Theory returns PECs along R_{S-H} similar to those shown for PhSMe in Figure 2b, though the energy barrier under CI-1 (from the $^1\pi\pi^*$(v = 0) level) is smaller.[29] Analyses of data recorded at different excitation wavelengths indicate photoexcitation to the $^1\pi\pi^*$ and $^1\pi\sigma^*$ states, prompt S−H bond fission on the $^1\pi\sigma^*$ PES (on a time scale that is short compared to the period of molecular rotation) and formation of both $\tilde{X}$ and $\tilde{A}$ state 4-MePhS radical products. Ultrafast pump−probe TA measurements following 267 nm excitation of 4-MePhSH in cyclohexane solution show an absorption centered at ∼480 nm appearing within the ∼100 fs instrument response time. This transient absorption is attributable to 4-MePhS($\tilde{X}$) radicals,[30,31] and signifies prompt photoinduced S−H bond rupture (as in the gas phase); it narrows and declines in amplitude with increasing pump−probe time delays, *t*. The narrowing reflects the dissipation of vibrational energy from the nascent radical products to the solvent bath, while the decreasing amplitude is a signature of geminate recombination. Careful scrutiny of the TA spectra reveals a feature at very early *t* attributable to 4-MePhS($\tilde{A}$) products—an outcome that, again, broadly mimics the gas phase photophysics. These electronically excited radicals are all quenched to their ground state by $t \sim 300$ fs.[32] Another absorption feature, at ∼380 nm, grows over a longer time scale, and shows the same kinetics as the (partial) decay of the 4-MePhS($\tilde{X}$) radical signal. This ∼380 nm band is attributable to a tautomer (cyclohexa-2,4- (or 2,5-) diene-1-thione) of 4-MePhSH formed by geminate recombination of the primary photoproducts.[30,31]

Time-resolved infrared (TRIR) absorption studies following 267 nm excitation of 4-MePhSH also reveal prompt formation of 4-MePhS($\tilde{X}$) radical products, with an out-of-equilibrium vibrational state population distribution.[33] Again, the evolving spectral profile reflects the relaxation of this product vibrational excitation through interaction with the solvent. The TRIR measurements also provide a direct probe of the parent ground state population. UV photoexcitation introduces "bleach" features in the IR TA spectrum, that partially recover with increasing *t*. This recovery confirms that geminate recombination leads not just to the above tautomer but also to some regeneration of the 4-MePhSH precursor. Nonetheless, the finding that the parent bleach does not fully recover indicates some "photodamage", and the late-time observation of 4-MePhS($\tilde{X}$) radical absorption confirms that some primary photoproducts escape the primary solvent cage and remain separated from the geminate partner.[33]

TRIR spectra taken following UV photolysis of 4-MePhSMe (in acetonitrile-d_3) show similarities, but also one notable difference.[33] As with 4-MePhSH, bleach features due to photoinduced depopulation of the parent S_0 state are evident at the earliest *t*, and a (weak) absorption attributable to 4-MePhS($\tilde{X}$) radicals (formed by S−Me bond fission in this case) grows with increasing *t*. However, these TRIR spectra also show another, intense, absorption attributable to 4-MePhSMe molecules in their $^1\pi\pi^*$ state. This excited state absorption shifts to higher frequencies at early *t* (reflecting the vibrational relaxation of the 4-MePhSMe($^1\pi\pi^*$) molecules) and decays to zero by $t \sim 1.5$ ns. Kinetic analysis returns solvent-dependent rate coefficients, but the principal findings are that the dissociation rate constant for 4-MePhSMe($^1\pi\pi^*$) molecules scales with the internal (vibrational) excitation and is always much smaller than that for 4-MePhSH($^1\pi\pi^*$) molecules.[33] Both findings mirror trends in excited state lifetime found in gas-phase studies of thiophenols and thioanisoles, and can be understood in light of the potential barrier associated with CI-1 (Figure 2b).

Dynamics of Photoinduced Ring-Opening in Solution. As already noted, orbital correlation arguments (Figure 4b) and *ab initio* theory (Figure 2c, and refs 23−25) suggest that $^1\pi\sigma^*$-state-mediated asymmetric ring-expansion constitutes a route by which photoexcited thiophene molecules can couple to the S_0 PES and ring-open. Stenrup[25] (and others[34]) have also identified a rival IC pathway initiated by out-of-plane deformation at the S atom, and qualitatively similar ring-puckered $^1\pi\pi^*/S_0$ CIs have also been reported for various substituted thiophenes.[35] Experimental studies capable of revealing the *dynamics* of photoinduced ring-opening processes are still in their infancy, however. The challenges are substantial. Near-UV photoexcitation of thiophene typically populates a $^1\pi\pi^*$ state. Such population can access the $^1\pi\sigma^*$ PES by nonadiabatic coupling in the region of CI-1, evolve toward CI-2 by extending R_{S-C} further, transfer to the S_0 PES and complete the ring-opening. The available experimental data[27] suggests that the initial coupling out of the $^1\pi\pi^*$ state (e.g., via CI-1) is an ultrafast process (<100 fs). Given the topography of the $^1\pi\sigma^*$ PES, the subsequent evolution toward CI-2 is also likely to occur on a time scale characteristic of a molecular vibration. The initial ring-opened species is an isomer of the starting heterocycle, so cannot be distinguished simply by mass spectrometric detection methods. The large geometry change upon ring-opening is likely to ensure that the products are formed with high levels of internal (vibrational) excitation. Indeed, the internal energy within the nascent ring-opened isomer(s) may well be sufficient to allow further isomerization, and even fragmentation. Without subsequent collisional relaxation, measurement and assignment of spectra of the ring-opened species are likely to be challenging.

Identifying a measurable that allows visualization of the early time dynamics is a challenge for experimental studies of photoinduced ring-opening. Hence the recent interest in substituted heterocycles carrying a "reporter" group whose spectral signature changes as the ring opens. Molecules like 2-thiophenone (Figure 1), for example, are well suited to study by ultrafast UV pump, broadband TRIR probe methods. As Figure 5a,f shows, the TRIR spectrum obtained following 267 nm photoexcitation of 2-thiophenone in acetonitrile displays an immediate parent bleach at ∼1685 cm^{-1} and a broad TA centered at ∼2150 cm^{-1}; the "reporter", the carbonyl vibration in 2-thiophenone, evolves into a ketene asymmetric stretch mode in the ring-opened product. The breadth of the latter feature, and its subsequent narrowing and shift to higher wavenumber, confirms prior expectations that the ring-opened product will be formed vibrationally excited and then relax (on a picosecond time scale) by coupling with the solvent bath. In this particular case, the decline in the amplitude of the parent bleach signal with increasing *t* implies that ∼60% of the photoexcited molecules ultimately ring-close again to reform 2-thiophenone.[36]

Results from similar UV-pump, TRIR absorption studies of four other carbonyl-bearing heterocycles—2(5H)-furanone (henceforth 2-furanone), *N*-methyl-2-pyridone, α-pyrone, and coumarin—are shown in Figure 5, along with their associated structures. The solvent in each case was acetonitrile. Relative to 2-thiophenone, the UV absorption spectrum of 2-furanone is

DOI: 10.1021/acs.jpclett.7b01219
J. Phys. Chem. Lett. 2017, 8, 3440−3451

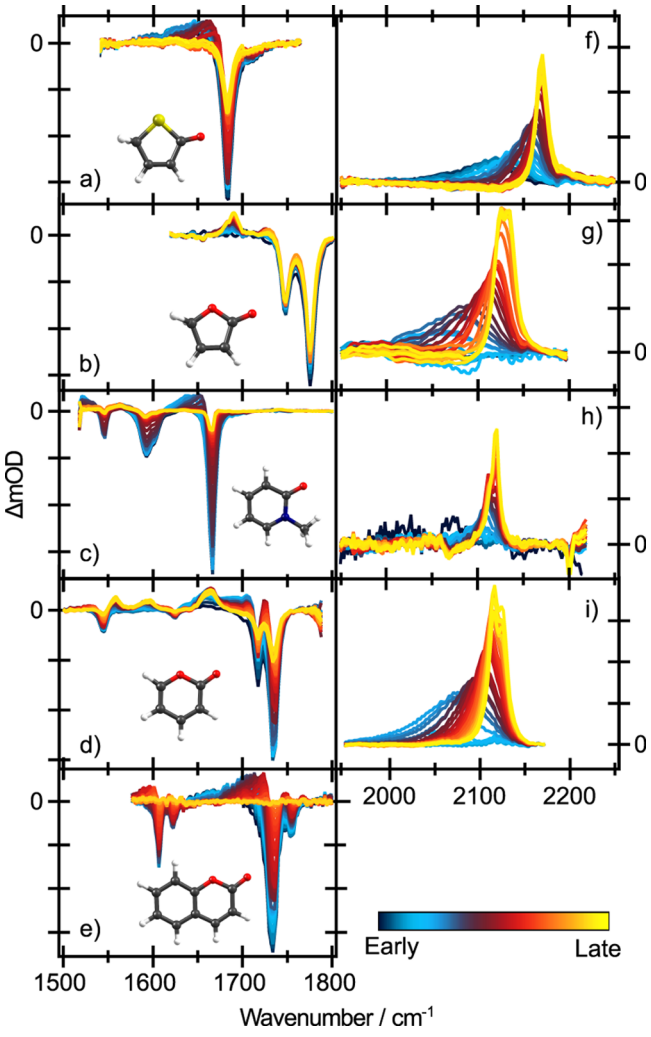

Figure 5. TRIR data for the 1500−1800 and 1950−2250 cm^{-1} regions following excitation of 2-thiophenone at 267 nm (panels a and f), 2-furanone at 225 nm (b and g), *N*-methyl-2-pyridone at 330 nm (c and h), α-pyrone at 310 nm (d and i) and coumarin at 330 nm (e), all in solution in acetonitrile, along with the corresponding equilibrium structures. These data are adapted from refs 36, 37, and 40, and are also displayed with the time delays specified in the Supporting Information.

shifted to shorter wavelengths, and the data shown here were recorded following 225 nm excitation. Photoinduced depletion of the ground state (i.e., ring closed) parent is revealed by the bleach signals centered at ∼1745 and 1775 cm^{-1} (Figure 5b) and the formation and subsequent vibrational relaxation of the ring-opened ketene is shown by the broad absorption that narrows and progressively shifts to an eventual center wavenumber of ∼2145 cm^{-1} (Figure 5g). Kinetic analysis of the time evolving bleach signals indicates that only ∼10% of the photoexcited species return to the S_0 state of 2-furanone.[36] Again, these solution phase studies are consistent with $^1\pi\sigma^*$-state mediated asymmetric ring expansion leading to the formation of ring-opened ketene products.

The electronic absorption spectrum of *N*-methyl-2-pyridone stretches to longer UV wavelengths than that of 2-thiophenone, and the displayed TRIR data were taken following excitation at 330 nm. Bleach features are again evident (Figure 5c), as is a developing absorption at ∼2120 cm^{-1} (Figure 5h).[37] However, the time scales are all much slower than in the cases of 2-thiophenone or 2-furanone; kinetic analyses return a parent excited state lifetime of ∼100 ps. Most (>90%) of the excited-state population returns to the parent S_0 state (i.e., *N*-methyl-2-pyridone is relatively photostable, like many N-containing heterocycles[38,39]). However, Figure 5c and 5h also shows that a small (≤10%) fraction of the photoexcited molecules react to form two ketenes, which are in equilibrium. The identity of these ketenes remains an open question. Initial analysis identified a prefulvenic CI between the S_1 and S_0 PESs with the C═O group out of the plane defined by the other five heavy atoms, encouraging suggestions that the ketene isomers arose via ring contraction,[37] but our more recent calculations identify two energetically accessible CIs between the S_1 and S_0 PESs characterized by extended N−C(O) bond lengths.

The remaining panels in Figure 5 show TRIR spectra measured following excitation of α-pyrone and coumarin (1,2-benzopyrone) at, respectively, 310 and 330 nm.[40] α-pyrone is another 6-membered heterocycle, but with an O atom adjacent to the carbonyl group; fusing α-pyrone with a benzene ring constitutes coumarin. Photoexcitation of α-pyrone yields the expected bleach signal in the carbonyl stretch region (Figure 5d), and an absorption that narrows and shifts to higher wavenumber (∼2120 cm^{-1}) with increasing t (Figure 5i). Again, this is the signature of vibrationally excited ketene products that "cool" by coupling with the surrounding solvent. Tracking the early time bleach recovery in the case of α-pyrone suggests an initial quantum yield $\phi \sim 0.68$ for IC and reformation of the parent in its S_0 state ($\phi \sim 0.60$ when photoexciting at 267 nm[41]). The ketene feature reveals the presence of at least two isomers, and temperature-dependent studies show that these undergo further (thermally driven $E \rightarrow Z$) isomerization processes that provide a (slower) route to eventual near-total recovery of the starting α-pyrone(S_0) population.[41]

Coumarin shows very different behavior. As Figure 5e shows, the parent S_0 molecule is reformed with essentially unit efficiency following excitation at 330 nm.[40] Yet the two lowest energy conical intersections (CI-a and CI-b) between the S_1 and S_0 states of α-pyrone and coumarin have remarkably similar geometries. Both involve O−C(O) bond extension and loss of planarity; the torsion angle between the carbonyl and ketene moieties at CI-a in both cases is ∼35°; at CI-b it is ∼90°.[40,42] PECs calculated along linearly interpolated internal coordinates linking the respective Franck−Condon regions (i.e., the geometries at which α-pyrone and coumarin are initially excited) and the respective CIs show no significant energy barriers to ring-opening. Intrinsic reaction coordinate analysis offers a rationale for the very different ring-opening probabilities. Such analyses, initialized at the CI-a and CI-b geometries, suggest that only CI-b in α-pyrone promotes ring-opening.[40] However, such analyses also remind us that knowledge of the nuclear geometry at a CI is necessary but generally is not sufficient information to allow prediction of the nuclear dynamics. *Ab initio* molecular dynamics (AIMD) simulations are finding growing use for exploring nonadiabatic excited state dynamics,[10,43,44] but applying such methods to systems like α-pyrone and coumarin is a challenge. In both cases, photoexcitation yields excited states with reported lifetimes in the psec range, which are likely to be subject to a range of nonadiabatic couplings with close-lying states both within the Franck−Condon region, and en route to and at CI-a and CI-b.[40,42,45] AIMD simulations thus require use of suitably high level electronic structure methods, long propagation times and, eventually, proper inclusion of solvent effects. Our work to date,

DOI: 10.1021/acs.jpclett.7b01219
J. Phys. Chem. Lett. 2017, 8, 3440−3451

involving just the isolated molecules, suggests that only in the case of CI-b in α-pyrone are the out-of-plane momenta sufficient to enable asymptotic ring-opening.

> Knowledge of the nuclear geometry at a CI is necessary but generally is not sufficient information to allow prediction of the nuclear dynamics.

These solution phase studies provide clear evidence for the formation of ring-opened ketene products following near UV photoexcitation of α-pyrone. Electronic structure calculations imply the operation of a similar asymmetric ring expansion following near UV photoexcitation of coumarin but, in this case, the forces acting during nonadiabatic coupling in the region of CI-a/b favor reformation of the ring-closed parent. Theory also reveals low energy CIs between the S_1 and S_0 PESs of *N*-methyl-2-pyridone characterized by N−C(O) bond extensions such as could lead to ring-opening, but the structures of the (minor yield) of ketene products formed following near UV photoexcitation of this molecule remain to be established.

It is now instructive to consider the extent to which the parent → product correlations shown for thiophene (Figure 4b) apply to the heterocycles featured in Figure 5. Following $\pi^* \leftarrow \pi$ excitation of 2-thiophenone or 2-furanone, efficient nonadiabatic coupling to the near-resonant $^1\pi\sigma^*$ PES (via CI-1) can direct population toward CI-2, where it transfers to the S_0 PES and eventual branches to either reform the ring-closed parent or form one or more ring-opened products.[36] There must be a rival $^1\pi\sigma^*$ PES that facilitates extension of the other S−C (O−C) bond in each of these molecules, but in both cases, the rival $^1\pi\sigma^*$ PES will lie at higher energy and correlate with less stable ring-opened products. The other molecules featured in Figure 5 show several important photophysical differences. The photoprepared states of 2-thiophenone and 2-furanone have lifetimes shorter than the ∼1 ps response time in the reported experiments, whereas the excited state lifetimes of α-pyrone and coumarin and of *N*-methyl-2-pyridone are in the few picoseconds and 100 ps ranges, respectively. Second, S−C(O) (O−C(O)) bond fission in 2-thiophenone or 2-furanone yields a biradical. One or more H atom migrations are then required en route to the experimentally observed ketenes, reminiscent of the thermal suprafacial/antarafacial [*n* + *m*]-sigmatropic shift reactions observed in many conjugated hydrocarbons.[46,47] Ketene formation following photoinduced N−C(O) bond fission in *N*-methyl-2-pyridone or O−C(O) bond fission in α-pyrone or coumarin, by contrast, would simply require an electrocyclic rearrangement; the nuclei are appropriately configured from the outset. These latter reactions show parallels with the photoinduced ring-opening of various cyclic-hydrocarbons, the outcomes of which accord with the Woodward−Hoffmann rules.[47,48] Such rules should be expected to extrapolate to, and describe, the photoinduced ring-opening of *N*-methyl-2-pyridine, α-pyrone, and coumarin also. Third, the first excited $^1\pi\pi^*$ states in these latter molecules all lie at much lower energy than the corresponding $^1\pi\pi^*$ state in 2-thiophenone or 2-furanone, i.e., the vertical energy separations between the lowest $^1\pi\pi^*$ and $^1\pi\sigma^*$ states in the featured six-membered heterocycles are substantially larger. This will reduce the probability of (and at sufficiently low excitation energies completely rule out) nonadiabatic coupling to the $^1\pi\sigma^*$ PES at the analogue of CI-1 as a route to asymmetric ring expansion following long wavelength $\pi^* \leftarrow \pi$ excitation of *N*-methyl-2-pyridone, α-pyrone, or coumarin.

This can also be illustrated with the help of schematic 4-electron orbital correlation diagrams such as that shown for α-pyrone in Figure 4c. The key orbitals in this case are the partially conjugated $2p_x(a'')$ orbital on the ring oxygen atom, a relatively low-lying excited $\pi^*(a'')$ orbital, and the bonding $\sigma_{O-C(O)}(a')$ and antibonding $\sigma_{O-C(O)}{}^*(a')$ orbitals localized on the extending bond. In this description, the S_0 parent molecule has the configuration $(a')^2(a'')^2$. The $^1\pi\pi^*$ state has configuration $(a')^2(a'')^1(a'')^1$ at planar geometries, but an appropriate combination of twisting and O−C(O) stretching motion provides an energetically feasible nonradiative route back to the S_0 state and possible ketene formation in the event of full O−C(O) bond fission.[40] Clearly, state labels like $^1\pi\pi^*$ progressively lose their meaning as the molecule distorts from planarity. The $^1\pi\sigma^*$ state, with configuration $(a')^2(a'')^1\sigma_{O-C(O)}{}^*(a')^1$, lies higher in energy and, importantly, correlates with an excited state ring-opened species, as illustrated in Figure 4c. The ring-opening revealed in Figure 5h,i, following near UV photoexcitation of *N*-methyl-2-pyridone and α-pyrone, can thus most plausibly be rationalized in terms of nonradiative coupling between the S_1 (predominantly $^1\pi\pi^*$) and S_0 states at distorted, twisted geometries. Such behavior is reminiscent of that shown following $\pi^* \leftarrow \pi$ excitation of 1,3-cyclohexadiene, for example, which undergoes a conrotatory ring-opening to form 1,3,5-hexatriene (*vide infra*) with an inherent stereochemistry that can be understood by means of an orbital energy and symmetry correlation diagram linking the reactant and product.[47] Such orbital correlation concepts can be expected to account for the out-of-plane ring-opening in α-pyrone also. The present analysis thus does not exclude a role for "classic" $^1\pi\sigma^*$-state mediated N−C(O) bond fission in *N*-methyl-2-pyridone (and O−C(O) bond fission in α-pyrone and, plausibly, coumarin), at shorter excitation wavelengths, to electronically excited ring-opened products, but this has yet to be demonstrated.

For completeness, we note that many of these same ring-opening processes had been previously recognized via IR spectroscopy measurements following prolonged broadband UV irradiation of, for example, 2-thiophenone, 2-furanone, and α-pyrone in an inert matrix.[49,50] The recent solution phase studies (and accompanying theory) give greater insight into the primary photochemistry, and the mechanisms and quantum yields of ring-opening,[33−37,40,41] but still cannot claim to be a direct probe of the ring-opening dynamics. Gas phase studies, allied with appropriate theory, offer the means of getting yet closer to this "holy grail".

Gas-Phase Studies of Photoinduced Ring-Opening. As noted earlier, the 193 nm PTS results for thiophene[26] are consistent with $^1\pi\sigma^*$-state mediated asymmetric ring expansion, nonadiabatic coupling to the S_0 PES and subsequent unimolecular decay. Recent imaging studies of the products formed by near UV photolysis of 2-bromothiophene (shown in Figure 1) and 2-iodothiophene provide further circumstantial evidence for photoinduced ring-opening in (substituted) thiophenes.[51] As Figure 6a shows, the image of the ground state Br atoms (detected by 2 + 1 REMPI) formed following ∼265 nm photoexcitation of 2-bromothiophene reveals a quite sharply defined, anisotropic velocity distribution. These products arise via prompt C−Br bond fission. Figure 6b shows an image of the partner thiophenyl radicals formed at a similar photolysis wavelength, and detected by 118 nm VUV ionization.[52]

DOI: 10.1021/acs.jpclett.7b01219
J. Phys. Chem. Lett. 2017, 8, 3440−3451

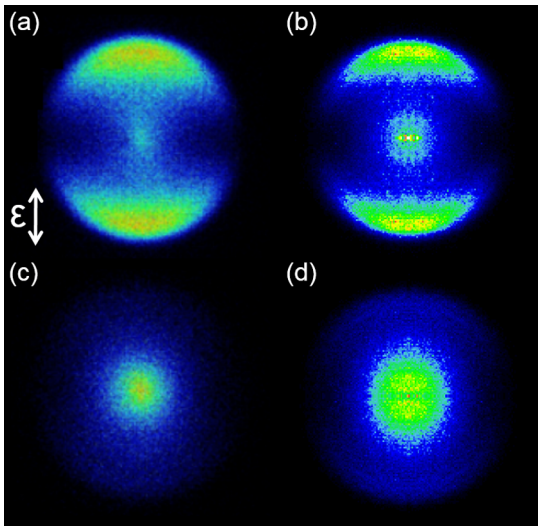

Figure 6. Br atom and partner C_4H_3S (m/z 83) fragment images from photolysis of jet-cooled gas phase 2-bromothiophene molecules at ~265 nm (a,b) and 245 nm (c,d). Data adapted from refs 51 and 52.

Reassuringly, this image shows the same recoil anisotropy, and the high velocity edge of its profile is momentum matched with that of the Br atoms. Analysis of these data reveal additional details including, for example, that the quantum yield for forming spin−orbit excited Br atoms at these wavelengths is small and that the slower thiophenyl fragments are underdetected in Figure 6b as a result of (unintended but unavoidable) dissociative photoionization by the 118 nm probe laser pulse.[52] In the present context, however, the corresponding data taken when exciting at ~245 nm (Figures 6c and 6d) are most noteworthy. Despite the increase in photon energy, the Br atom and partner m/z 83 radical images are both much smaller, and isotropic.[51,52] Companion electronic structure calculations suggest that this evolving behavior reflects the onset of a rival excited state decay pathway, involving $\pi\sigma^*$-state mediated asymmetric S−C(Br) bond extension, nonadiabatic coupling to the S_0 PES and formation of one or more excited ring-opened isomers with sufficient internal energy to exceed the energetic threshold for unimolecular decay and loss of a (slow) Br atom.[51]

The oxygen-containing analogue of thiophene is furan. PTS studies of furan following excitation at 193 nm identified three fragmentation pathways (a radical channel giving C_3H_3 + HCO products, and two molecular channels yielding, respectively, C_3H_4 + CO and H_2CCO + C_2H_2).[53] These observations, and the respective product energy disposals, were rationalized by invoking photoinduced ring-opening and subsequent unimolecular decay of the ring-opened species, but it was several years before the ultrafast excited state decay dynamics following excitation at 200 nm were explored by time-resolved photoelectron spectroscopy (TRPES),[54] and $\pi\sigma^*$-state mediated asymmetric ring expansion identified as a nuclear distortion capable of driving nonadiabatic coupling to the S_0 PES.[55] As Figure 7a shows, the calculated PECs along this O−C elongation coordinate leading to CI-2 in (planar) furan are very similar to those for the analogous asymmetric expansion in thiophene (Figure 2c). As in thiophene,[25] theory also identifies a rival CI in furan with a ring-puckered geometry, which could also promote IC to the S_0 state.[56,57] Ultrafast TRPES studies of furan suggest that the excited-state population formed by 200 nm photoexcitation returns to the S_0 state within ~100 fs,

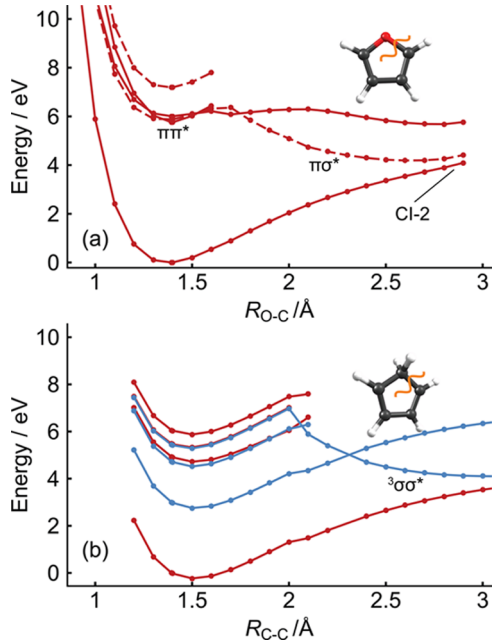

Figure 7. Calculated PECs for (a) the S_0 and lowest excited singlet states of furan along an R_{O-C} ring-opening coordinate and (b) the S_0 and lowest excited singlet (shown in red) *and* triplet (in blue) states of 1,3-cyclopentadiene along the corresponding R_{C-C} ring-opening coordinate. All ring atoms are constrained to lie in a plane, and solid and dashed lines are used to distinguish states of A' and A'' symmetry, respectively. Further details are provided in the Supporting Information.

and accompanying molecular dynamics simulations suggest contributions from both IC pathways.[58]

Other notable recent studies include a theoretical work proposing $\sigma^* \leftarrow \pi$ excitation as a driver for O−C bond fission (i.e., ring-opening) in a spiropyran,[59] and an *ab initio* study of the excited state photophysics of a carbohydrate molecule (β-D-glucopyranose) that predicts both $^1n\sigma^*$-state-mediated O−C bond fission (i.e., ring-opening) and $^1n\sigma^*$-state-mediated fission of the pendant O−H bonds.[60] The saturation of the carbohydrate molecule is attractive in the present context, as it greatly reduces the range of possible orbital promotions. It is tempting to suggest that similar $\sigma^* \leftarrow n$ excitations could trigger O−C bond extension, IC to the S_0 state, and the eventual fragmentation reported following 193 nm photoexcitation of the cyclic ethers oxetane[61] and tetrahydrofuran.[62] An early theoretical study of photoinduced ring-opening of oxirane also hinted at such a mechanism.[63]

Pyrrole and 1,3-cyclopentadiene are isoelectronic with furan, but these unsaturated 5-membered cyclic systems show quite distinctive excited state photophysics. The near UV photochemistry of pyrrole is dominated by prompt N−H bond fission following excitation from the (π) HOMO to a σ^* orbital localized on the N−H bond.[13,64] TRPES studies at these near UV wavelengths return excited state lifetimes of ~20 fs.[65] Other excited states are accessed upon tuning to shorter wavelengths; these excited states decay more slowly, by nonadiabatic coupling to the $^1\pi\sigma_{N-H}^*$-continuum and N−H bond fission, and by rival nonradiative decay pathways to the S_0 PES and subsequent unimolecular decay. The latter processes are revealed via an increased yield of slow H atoms and of products other than H + pyrrolyl fragments.[66] Theory identifies CIs involving both ring-puckered and asymmetric ring-expanded

DOI: 10.1021/acs.jpclett.7b01219
J. Phys. Chem. Lett. 2017, 8, 3440−3451

geometries, but these dissociation pathways involving heavy atom distortions struggle to compete with the ultrafast N−H bond fission process.[67] The latter can be slowed by substituting a Me group in place of the H atom. Studies of *N*-methylpyrrole reveal formation of translationally excited Me products, on a hundreds of picoseconds time scale, when exciting at wavelengths in the range 240−250 nm (i.e., to the $^1\pi\sigma_{N-Me}$*-continuum).[68,69] Tuning to shorter wavelengths, the excited state lifetime drops substantially, and the Me fragments display a slow, essentially "statistical" kinetic energy distribution. Such observations have been rationalized by invoking the onset of a rival fast population loss process (IC to the S_0 state driven by ring-puckering and/or asymmetric ring-expansion) and subsequent unimolecular decay.[68,69] Excited-state photophysics similar to that for pyrrole has been predicted for imidazole[70] where, again, IC via CIs involving both ring-puckered and asymmetric ring-expanded geometries have been identified as potential competitors to N−H bond fission[71] at higher excitation energies.

Unlike the O atom in furan or the N atom in pyrrole, the corresponding (sp^3 hybridized) C atom in 1,3-cyclopentadiene supports no π electrons. As Figure 7b shows, the ring-opened biradical in this case associates with just one singlet PES (which correlates with the S_0 state of the ring closed molecule) and a repulsive triplet potential. The $^1\pi\sigma$* state correlates to an electronically excited state of the biradical, and cannot mediate nonadiabatic coupling to the S_0 PES by appropriate elongation of the C1−C5 bond. Rather, theory (AIMD simulations)[72] and experiment (TRPES)[72,73] both suggest that the ultrafast nonradiative decay following $\pi^* \leftarrow \pi$ excitation in 1,3-cyclopentadiene involves initial (in-plane) motion along the bond-alternation coordinate followed by out-of-plane torsional motion about the C=C double bonds (reminiscent of the nuclear motions following $\pi^* \leftarrow \pi$ excitation of ethene[74]) so as to access regions of CI with the S_0 PES. The eventual fate of the resulting highly vibrationally excited S_0 molecules in a collision-free gas phase experiment remains an open question.

The photoinduced ring-opening of 1,3-cyclohexadiene has been studied more extensively.[75−83] As with 1,3-cyclopentadiene, near UV absorption results in population of a "bright" $^1\pi\pi$* excited state. A recent TRPES study[82] questions the previous consensus view that the very early time dynamics following photoexcitation involves nonradiative coupling to an optically dark (2A) state. Thereafter, however, there is little doubt that the topography of the excited state PES(s) encourages C5−C6 bond extension and torsion around the C=C double bonds, thereby priming the molecule for radiationless transfer though a CI with the S_0 state and full ring-opening (to 1,3,5-hexatriene) or reversion to the ring-closed starting molecule. Again, the valency of the relevant C atoms in 1,3-cyclohexadiene is saturated, so there is no $^1\pi\sigma$* excited state to promote any rival nonadiabatic coupling pathway to the S_0 PES by C5−C6 bond extension.

Conclusions and Prospects. The recent literature contains many experimental and theoretical demonstrations of near UV photoinduced bond fission in heteroatom containing molecules following population of a $^1\pi\sigma$* excited state.[13] Theory points to the likelihood of analogous $^1\pi\sigma$*-state-mediated bond fission as a ring-opening mechanism in heterocycles,[24,25,28,55,56,58] and there is a growing body of experimental literature illustrating near-UV photoinduced ring-opening in such molecules.[33,36,37,40,41,51,52] The initial absorption in most systems studied to date involves a $\pi^* \leftarrow \pi$ excitation, however, and it remains a challenge to confirm whether an observed ring-opening is driven by nonadiabatic coupling to, first, the $^1\pi\sigma$*-state and then, after further asymmetric ring-expansion, to the S_0 PES, rather than by a rival $^1\pi\pi^*/S_0$ coupling enabled by suitable out-of-plane distortions.

$^1\pi\sigma_{X-C}$*-state (X = S, O)-mediated bond fission is argued to play an important role in the ultrafast ring-opening of the 5-membered heterocycles thiophene and furan, and analogues like 2-thiophenone, 2-furanone, and 2-bromo- and 2-iodothiophene, but the recently observed near UV photoinduced ring-opening of *N*-methyl-2-pyridone and α-pyrone is more likely driven by nonadiabatic coupling at CIs between the $^1\pi\pi$* and S_0 PESs at nonplanar geometries. Comparisons between α-pyrone and coumarin serve to emphasize the importance of both structure *and dynamics* in determining the nonadiabatic coupling probability at any given CI, and to highlight the challenges of realistic dynamical calculations involving such systems. *N*-methyl-2-pyridone, α-pyrone, and coumarin must possess $^1\pi\sigma_{X-C}$* (X = N, O) states, but these will typically lie at higher energies than have been investigated to date. The $^1\pi\sigma$* states in these latter heterocycles all correlate with an excited state of the ring-opened species, so ring-opening may not be an exoergic option following near UV photoexcitation. Such energetic constraints are likely to fade in importance on tuning to shorter (vacuum) UV excitation wavelengths, however, where electron promotions to the appropriate bond localized σ* orbital (and from bond localized σ orbitals) are both likely to exhibit progressively larger partial absorption cross sections.

Apart from its intrinsic photophysical interest, 1,3-cyclohexadiene has also been a popular test system for demonstrating new experimental routes for probing the dynamics of photoinduced ring-opening. The works cited at the end of the previous section include early examples of ultrafast condensed phase pump−probe studies,[75] ultrafast transient ionization studies,[77] TRPES[79,80,82] and femtosecond X-ray spectroscopy studies,[81,83] all of which either have been, or soon can be expected to be, applied to the various types of asymmetric ring expansion and heterocyclic ring-opening featured in this Perspective. To this growing armory of techniques, one can also anticipate growing interest in the use of Coulomb explosion imaging methods. Correlations and/or covariances revealed using such methods have already been shown to offer a direct probe of the photoinduced torsional dynamics of strategically substituted biphenyl derivatives on their ground-state PES[84] and are now starting to find use in probing photoisomerizations[85−87] and excited state bond fission processes.[88]

■ ASSOCIATED CONTENT

Ⓢ Supporting Information

The Supporting Information is available free of charge on the ACS Publications website at DOI: 10.1021/acs.jpclett.7b01219.

Details of the calculation of potential energy profiles for the ground and various excited states of dimethylsulfide, thioanisole, thiophene, furan, and 1,3-cyclopentadiene along the chosen bond extension coordinate (R_i); Figure 5 data, displayed on an expanded scale and with the various time delays specified (PDF)

■ AUTHOR INFORMATION

Corresponding Author

*E-mail: mike.ashfold@bristol.ac.uk.

DOI: 10.1021/acs.jpclett.7b01219
J. Phys. Chem. Lett. 2017, 8, 3440−3451

ORCID

Michael N. R. Ashfold: 0000-0001-5762-7048

Present Addresses

[†]Department of Chemistry, Temple University, 13th and Norris Streets, Philadelphia, PA 19122, U.S.A.

[‡]Department of Chemistry, University of Pennsylvania, 231 S. 34 Street, Philadelphia, PA 19104-6323, U.S.A.

[§]Department of Chemistry, University of Warwick, Gibbet Hill Road, Coventry, U.K., CV4 7AL.

Notes

The authors declare no competing financial interest.

Biographies

Mike Ashfold obtained his Ph.D. degree in the group of Prof. John Simons (University of Birmingham). Following postdoctoral research at Oxford University, he was appointed as a Lecturer at the University of Bristol, where he was promoted to a Chair in Physical Chemistry in 1992. He was elected to the Fellowship of the Royal Society in 2009. His research interests include gas and solution phase molecular photophysics and spectroscopy.

Matthew Bain completed his M.Chem. degree at Heriot Watt University in Edinburgh, and began Ph.D. studies in the Ashfold group in 2015. His Ph.D. research focuses on the application of multimass velocity ion map imaging to problems in molecular photochemistry.

Christopher Hansen completed his Ph.D. (2015) at the University of Wollongong in the group of Assoc. Prof. Adam Trevitt, where he explored the photodissociation, spectroscopy, and reactivity of heterocyclic cations in an ion trap mass spectrometer. He accepted a postdoctoral position in the groups of Profs. Ashfold and Andrew Orr-Ewing at Bristol in early 2016, where his research centers on applying fast-framing CMOS sensors and universal detection methods to multimass velocity map imaging and studies of molecular photodissociation dynamics.

Rebecca Ingle earned her M.Chem. degree from the University of York, and is now finishing her Ph.D. degree in the Ashfold group at Bristol. She spent parts of the summers of 2014 and 2015 working in the group of Prof. Toshinori Suzuki at Kyoto University, during which time she also engaged with the computational chemistry group of Prof. Satoshi Maeda at the University of Hokkaido. Rebecca's research spans all aspects of excited state dynamics—experimental and computational, in the gas and solution phase.

Tolga Karsili obtained his Ph.D. in 2014 from the University of Bristol, then undertook postdoctoral research at the Technical University of Munich, Germany (supported by a T.U. Munich Fellowship) and is now a research fellow at Temple University. His research interests involve the excited state chemistry of organic and biological chromophores, supramolecular photochemistry, and electron-induced reactions in both the gas and solution phases.

Barbara Marchetti earned Bachelor and Masters degrees at the Università degli Studi di Perugia, a Ph.D. from the University of Bristol (2016), and is now a Marie Skłodowska Curie International Postdoctoral Research Fellow in the group of Prof. Marsha Lester at the University of Pennsylvania. Her research interests include the photochemistry and photophysics of biologically, catalytically, and environmentally relevant chromophores.

Dan Murdock obtained his M.Chem. degree in Chemistry from the University of Durham, then undertook Ph.D. research in the group of Prof. Pat Vaccaro at Yale University before moving to a postdoctoral research position with Profs. Ashfold and Orr-Ewing at Bristol in 2009. He was appointed as a Teaching Fellow in Physical Chemistry at the University of Warwick in early 2017.

ACKNOWLEDGMENTS

The authors are grateful to the Engineering and Physical Sciences Research Council for funding through a Programme Grant (EP/L005913).

REFERENCES

(1) Schafer, F. P., Ed. *Dye Lasers*, 3rd ed.; Springer-Verlag: Berlin, 1990.

(2) Sauer, M.; Hofkens, J.; Enderlein, J. *Handbook of Fluorescence Spectroscopy and Imaging*; Wiley-VCH Verlag GmbH & Co. KGaA: Weinheim, Germany, 2011.

(3) Weiss, S. Fluorescence Spectroscopy of Single Biomolecules. *Science* **1999**, *283*, 1676−1683.

(4) Huang, B.; Bates, M.; Zhuang, X. W. Super-Resolution Fluorescence Microscopy. *Annu. Rev. Biochem.* **2009**, *78*, 993−1016.

(5) Hell, S. W. Far-field Optical Nanoscopy. *Science* **2007**, *316*, 1153−1158.

(6) Middleton, C. T.; de la Harpe, K.; Su, C.; Law, Y. K.; Crespo-Hernandez, C. E.; Kohler, B. DNA Excited-State Dynamics: From Single Bases to the Double Helix. *Annu. Rev. Phys. Chem.* **2009**, *60*, 217−239.

(7) Baker, L. A.; Marchetti, B.; Karsili, T. N. V.; Stavros, V. G.; Ashfold, M. N. R. Photoprotection: Extending Lessons Learned from Studying Natural Sunscreens to the Design of Artificial Sunscreen Constituents. *Chem. Soc. Rev.* **2017**, *46*, 3770−3791.

(8) Bernardi, F.; Olivucci, M.; Robb, M. A. Potential Energy Surface Crossings in Organic Photochemistry. *Chem. Soc. Rev.* **1996**, *25*, 321−328.

(9) Worth, G. A.; Cederbaum, L. S. Beyond Born-Oppenheimer: Molecular Dynamics through a Conical Intersection. *Annu. Rev. Phys. Chem.* **2004**, *55*, 127−158.

(10) Levine, B. G.; Martinez, T. J. Isomerization through Conical Intersections. *Annu. Rev. Phys. Chem.* **2007**, *58*, 613−634.

(11) Matsika, S.; Krause, P. Nonadiabatic Events and Conical Intersections. *Annu. Rev. Phys. Chem.* **2011**, *62*, 621−643.

(12) Domcke, W.; Yarkony, D. R. Role of Conical Intersections in Molecular Spectroscopy and Photoinduced Chemical Dynamics. *Annu. Rev. Phys. Chem.* **2012**, *63*, 325−352.

(13) Ashfold, M. N. R.; King, G. A.; Murdock, D.; Nix, M. G. D.; Oliver, T. A. A.; Sage, A. G. $\pi\sigma^*$ States in Molecular Photochemistry. *Phys. Chem. Chem. Phys.* **2010**, *12*, 1218−1238.

(14) Limão-Vieira, P.; Eden, S.; Kendall, P. A.; Mason, N. J.; Hoffmann, S. V. High Resolution VUV Photo-Absorption Cross-Sction for Dimethylsulphide, $(CH_3)_2S$. *Chem. Phys. Lett.* **2002**, *366*, 343−349.

(15) Yoon, J.-H.; Woo, K. C.; Kim, S. K. Vibronic Structures and Dynamics of the Predissociating Dimethyl Sulfide and its Isotopomers (CH_3SCH_3, CD_3SCD_3, CH_3SCD_3) at the Conical Intersection. *Phys. Chem. Chem. Phys.* **2014**, *16*, 8949−8955.

(16) Martinez-Haya, B.; Quintana, P.; Banares, L.; Samartzis, P.; Smith, D. J.; Kitsopoulos, T. N. The Photodissociation of CH_3SCH_3 and CD_3SCD_3 at 220−231 nm Investigated by Velocity Map Ion Imaging. *J. Chem. Phys.* **2001**, *114*, 4450−4456.

(17) Lim, J. S.; Kim, S. K. Experimental Probing of Conical Intersection Dynamics in the Photodissociation of Thioanisole. *Nat. Chem.* **2010**, *2*, 627−632.

(18) Han, S.; Lim, J. S.; Yoon, J. H.; Lee, J.; Kim, S. Y.; Kim, S. K. Conical Intersection Seam and Bound Resonances Embedded in Continuum Observed in the Photodissociation of Thioanisole-d_3. *J. Chem. Phys.* **2014**, *140*, 054307.

(19) Roberts, G. M.; Hadden, D. L.; Bergendahl, L. T.; Wenge, A. M.; Harris, S. J.; Karsili, T. N. V.; Ashfold, M. N. R.; Paterson, M. J.; Stavros, V. G. Exploring Quantum Phenomena and Vibrational Control in σ^* Mediated Photochemistry. *Chem. Sci.* **2013**, *4*, 993−1001.

(20) Wenge, A. M.; Karsili, T. N. V.; Rodriguez, J. D.; Cotterell, M. I.; Marchetti, B.; Dixon, R. N.; Ashfold, M. N. R. Tuning Photochemistry:

DOI: 10.1021/acs.jpclett.7b01219
J. Phys. Chem. Lett. 2017, 8, 3440−3451

Substituent Effects on $n\pi^*$ State Mediated Bond Fission in Thioanisoles. *Phys. Chem. Chem. Phys.* **2015**, *17*, 16246−16256.
(21) Li, S. L.; Truhlar, D. G. Full-dimensional Ground- and Excited-State Potential Energy Surface and State Couplings for Photodissociation of Thioanisole. *J. Chem. Phys.* **2017**, *146*, 064301.
(22) Hoshino-Nagasaka, M.; Suzuki, T.; Ichimura, T.; Kasahara, S.; Baba, M.; Kawauchi, S. Rotationally Resolved High-resolution Spectrum of the S_1−S_0 Transition of Jet-cooled Thioanisole. *Phys. Chem. Chem. Phys.* **2010**, *12*, 13243−13247.
(23) Salzmann, S.; Kleinschmidt, M.; Tatchen, J.; Weinkauf, R.; Marian, C. M. Excited States of Thiophene: Ring Opening as Deactivation Mechanism. *Phys. Chem. Chem. Phys.* **2008**, *10*, 380−392.
(24) Cui, G. L.; Fang, W. H. Ab Initio Trajectory Surface-Hopping Study on Ultrafast Deactivation Process of Thiophene. *J. Phys. Chem. A* **2011**, *115*, 11544−11550.
(25) Stenrup, M. Theoretical Study of the Radiationless Deactivation Mechanisms of Photo-Excited Thiophene. *Chem. Phys.* **2012**, *397*, 18−25.
(26) Qi, F.; Sorkhabi, O.; Rizvi, A. H.; Suits, A. G. 193 nm Photodissociation of Thiophene Probed Using Synchrotron Radiation. *J. Phys. Chem. A* **1999**, *103*, 8351−8358.
(27) Weinkauf, R.; Lehr, L.; Schlag, E. W.; Salzmann, S.; Marian, C. M. Ultrafast Dynamics in Thiophene by Femtosecond Pump Probe Photoelectron Spectroscopy and Theory. *Phys. Chem. Chem. Phys.* **2008**, *10*, 393−404.
(28) Wu, X. F.; Zheng, X. M.; Wang, H. G.; Zhao, Y. Y.; Guan, X. G.; Phillips, D. L.; Chen, X. B.; Fang, W. H. A Resonance Raman Spectroscopic and CASSCF Investigation of the Franck-Condon Region Structural Dynamics and Conical Intersections of Thiophene. *J. Chem. Phys.* **2010**, *133*, 134507.
(29) Oliver, T. A. A.; King, G. A.; Tew, D. P.; Dixon, R. N.; Ashfold, M. N. R. Controlling the Electronic Product Branching at Conical Intersections in the UV Photolysis of *para*-Substituted Thiophenols. *J. Phys. Chem. A* **2012**, *116*, 12444−12459.
(30) Oliver, T. A. A.; Zhang, Y.; Ashfold, M. N. R.; Bradforth, S. E. Linking Photochemistry in the Gas and Solution Phase: S−H Bond Fission in *p*-Methylthiophenol Following UV Photoexcitation. *Faraday Discuss.* **2011**, *150*, 439−458.
(31) Zhang, Y.; Oliver, T. A. A.; Ashfold, M. N. R.; Bradforth, S. E. Contrasting the Excited State Reaction Pathways of Phenol and para-Methylthiophenol in the Gas and Liquid Phases. *Faraday Discuss.* **2012**, *157*, 141−163.
(32) Zhang, Y.; Oliver, T. A. A.; Das, S.; Roy, A.; Ashfold, M. N. R.; Bradforth, S. E. Exploring the Energy Disposal Immediately after Bond-Breaking in Solution: The Wavelength-Dependent Excited State Dissociation Pathways of para-Methylthiophenol. *J. Phys. Chem. A* **2013**, *117*, 12125−12137.
(33) Murdock, D.; Harris, S. J.; Karsili, T. N. V.; Greetham, G. M.; Clark, I. P.; Towrie, M.; Orr-Ewing, A. J.; Ashfold, M. N. R. Photofragmentation Dynamics in Solution Probed by Transient IR Absorption Spectroscopy: $\pi\sigma^*$-Mediated Bond Cleavage in *p*-Methylthiophenol and *p*-Methylthioanisole. *J. Phys. Chem. Lett.* **2012**, *3*, 3715−3720.
(34) Prlj, A.; Curchod, B. F. E.; Corminboeuf, C. Excited State Dynamics of Thiophene and Bithiophene: New Insights into Theoretically Challenging Systems. *Phys. Chem. Chem. Phys.* **2015**, *17*, 14719−14730.
(35) Su, M.-D. *J. Comput. Chem.* **2010**, *31*, 43−56.
(36) Murdock, D.; Harris, S. J.; Luke, J.; Grubb, M. P.; Orr-Ewing, A. J.; Ashfold, M. N. R. Transient UV-Pump-IR Probe Investigation of Heterocyclic Ring-Opening Dynamics in the Solution Phase: The Role Played by $n\sigma^*$ States in the Photoinduced Reactions of Thiophenone and Furanone. *Phys. Chem. Chem. Phys.* **2014**, *16*, 21271−21279.
(37) Murdock, D.; Harris, S. J.; Clark, I. P.; Greetham, G. M.; Towrie, M.; Orr-Ewing, A. J.; Ashfold, M. N. R. UV-Induced Isomerization Dynamics of N-Methyl-2-Pyridone in Solution. *J. Phys. Chem. A* **2015**, *119*, 88−94.
(38) Crespo-Hernández, C. E.; Cohen, B.; Hare, P. M.; Kohler, B. Ultrafast Excited-State Dynamics in Nucleic Acids. *Chem. Rev.* **2004**, *104*, 1977−2019.
(39) Marchetti, B.; Karsili, T. N. V.; Ashfold, M. N. R.; Domcke, W. A 'Bottom Up', *Ab Initio* Computational Approach to Understanding Fundamental Photophysical Processes in Nitrogen Containing Heterocycles, DNA Bases and Base-Pairs. *Phys. Chem. Chem. Phys.* **2016**, *18*, 20007−20027.
(40) Murdock, D.; Ingle, R. A.; Sazanovich, I. V.; Clark, I. P.; Harabuchi, Y.; Taketsugu, T.; Maeda, S.; Orr-Ewing, A. J.; Ashfold, M. N. R. Contrasting Ring-Opening Propensities in UV-Excited α-Pyrone and Coumarin. *Phys. Chem. Chem. Phys.* **2016**, *18*, 2629−2638.
(41) Murdock, D.; Clark, I. P.; Ashfold, M. N. R. Probing Photochemically and Thermally Induced Isomerization Reactions in α-Pyrone. *J. Phys. Chem. A* **2016**, *120*, 7249−7254.
(42) Maeda, S.; Harabuchi, Y.; Taketsugu, T.; Morokuma, K. Systematic Exploration of Minimum Energy Conical Intersection Structures near the Franck−Condon Region. *J. Phys. Chem. A* **2014**, *118*, 12050−12058.
(43) Lasorne, B.; Worth, G. A.; Robb, M. A. Excited-State Dynamics. *Wiley Interdiscip. Rev. Comput. Mol. Sci.* **2011**, *1*, 460−475.
(44) Tavernelli, I. Nonadiabatic Molecular Dynamics Simulations: Synergies between Theory and Experiments. *Acc. Chem. Res.* **2015**, *48*, 792−800 and references therein..
(45) Krauter, C. M.; Möhring, J.; Buckup, T.; Pernpointner, M.; Motzkus, M. Ultrafast Branching in the Excited State of Coumarin and Umbelliferone. *Phys. Chem. Chem. Phys.* **2013**, *15*, 17846−17861.
(46) Kiefer, E. F.; Tanna, C. H. Alternative Electrocyclic Pathways. Photolysis and Thermolysis of Dimethylallene Dimers. *J. Am. Chem. Soc.* **1969**, *91*, 4478−4480.
(47) Woodward, R. B.; Hoffmann, R. *The Conservation of Orbital Symmetry*; Verlag Chemie/Academic Press: Weinheim/New York, 1971.
(48) Winter, R. E. K. Preparation and Isomerization of Cis- and Trans-3,4-Dimethylcyclobutene. *Tetrahedron Lett.* **1965**, *6*, 1207−1212.
(49) Breda, S.; Reva, I.; Fausto, R. UV-Induced Unimolecular Photochemistry of 2(5H)-Furanone and 2(5H)-Thiophenone Isolated in Low Temperature Inert Matrices. *Vib. Spectrosc.* **2009**, *50*, 57−67.
(50) Breda, S.; Reva, I.; Lapinski, L.; Fausto, R. Matrix Isolation FTIR and Theoretical Study of a-Pyrone Photochemistry. *Phys. Chem. Chem. Phys.* **2004**, *6*, 929−937.
(51) Marchetti, B.; Karsili, T. N. V.; Kelly, O.; Kapetanopoulos, P.; Ashfold, M. N. R. Near Ultraviolet Photochemistry of 2-Bromo- and 2-Iodothiophene: Revealing Photoinduced Ring Opening in the Gas Phase? *J. Chem. Phys.* **2015**, *142*, 224303.
(52) Ingle, R. A.; Hansen, C. S.; Elsdon, E.; Bain, M.; King, S. J.; Lee, J. W. L.; Brouard, M.; Vallance, C.; Turchetta, R.; Ashfold, M. N. R. Ultraviolet Photochemistry of 2-Bromothiophene Explored using Universal Ionization Detection and Multi-Mass Velocity-Map Imaging with a PImMS2 Sensor. *J. Chem. Phys.* **2017**, *147*, 013914.
(53) Sorkhabi, O.; Qi, F.; Rizvi, A. H.; Suits, A. G. Ultraviolet Photodissociation of Furan Probed by Tunable Synchrotron Radiation. *J. Chem. Phys.* **1999**, *111*, 100−107.
(54) Fuji, T.; Suzuki, Y.-I.; Horio, T.; Suzuki, T.; Mitrić, R.; Werner, U.; Bonačić-Koutecky, V. Ultrafast Photodynamics of Furan. *J. Chem. Phys.* **2010**, *133*, 234303.
(55) Gavrilov, N.; Salzmann, S.; Marian, C. M. Deactivation via Ring Opening: A Quantum Chemical Study of the Excited States of Furan and Comparison to Thiophene. *Chem. Phys.* **2008**, *349*, 269−277.
(56) Stenrup, M.; Larson, A. A Computational Study of Radiationless Deactivation Mechanisms of Furan. *Chem. Phys.* **2011**, *379*, 6−12.
(57) Gromov, E. V.; Lévêque, C.; Gatti, F.; Burghardt, I.; Köppel, H. Ab Initio Quantum Dynamical Study of Photoinduced Ring Opening in Furan. *J. Chem. Phys.* **2011**, *135*, 164305.
(58) Oesterling, S.; Schalk, O.; Geng, T.; Thomas, R. D.; Hansson, T.; de Vivie-Riedle, R. Substituent Effects on the Relaxation Dynamics of Furan, Furfural and β-Furfural: A Combined Theoretical and

DOI: 10.1021/acs.jpclett.7b01219
J. Phys. Chem. Lett. 2017, 8, 3440−3451

Experimental Approach. *Phys. Chem. Chem. Phys.* **2017**, *19*, 2025−2035.
(59) Liu, F.; Morokuma, K. Multiple Pathways for the Primary Step of the Spiropyran Photochromic Reaction: A CASPT2/CASSCF Study. *J. Am. Chem. Soc.* **2013**, *135*, 10693−10702.
(60) Tuna, D.; Sobolewski, A. L.; Domcke, W. Electronically Excited States and Photochemical Reaction Mechanisms of β-glucose. *Phys. Chem. Chem. Phys.* **2014**, *16*, 38−47.
(61) Lee, S.-H. The Photodissociation of Oxetane at 193 nm as the Reverse of the Paterno-Buchi Reaction. *J. Chem. Phys.* **2009**, *131*, 224309.
(62) Lee, S.-H. Dynamics of Multi-Channel Dissociation of Tetrahydrofuan Photoexcited at 193 nm: Distributions of Kinetic Energy, Angular Anisotropies and Branching Ratios. *Phys. Chem. Chem. Phys.* **2010**, *12*, 2655−2663.
(63) Tapavicza, E.; Tavernelli, I.; Rothlisberger, U.; Filippi, C.; Casida, M. E. Mixed Time-Dependent Density-Functional Theory/Classical Trajectory Surface Hopping Study of Oxirane Photochemistry. *J. Chem. Phys.* **2008**, *129*, 124108.
(64) Cronin, B.; Nix, M. G. D.; Qadiri, R. H.; Ashfold, M. N. R. High Resolution Photofragment Translational Spectroscopy Studies of the Near Ultraviolet Photolysis of Pyrrole. *Phys. Chem. Chem. Phys.* **2004**, *6*, 5031−5041.
(65) Wu, G. R.; Neville, S. P.; Schalk, O.; Sekikawa, T.; Ashfold, M. N. R.; Worth, G. A.; Stolow, A. Excited State Non-Adiabatic Dynamics of Pyrrole: A Time-Resolved Photoelectron Spectroscopy and Quantum Dynamics Study. *J. Chem. Phys.* **2015**, *142*, 074302 and references therein..
(66) Blank, D. A.; North, S. W.; Lee, Y. T. The Ultraviolet Photodissociation Dynamics of Pyrrole. *Chem. Phys.* **1994**, *187*, 35−47.
(67) Barbatti, M.; Pittner, J.; Pederzoli, M.; Werner, U.; Mitric, R.; Bonacic-Koutecky, V.; Lischka, H. Non-Adiabatic Dynamics of Pyrrole: Dependence of Deactivation Mechanisms on the Excitation Energy. *Chem. Phys.* **2010**, *375*, 26−34.
(68) Sage, A. G.; Nix, M. G. D.; Ashfold, M. N. R. UV Photodissociation of N-Methylpyrrole: The Role of $^1\pi\sigma^*$ States in Non-Hydride Heteroaromatic Systems. *Chem. Phys.* **2008**, *347*, 300−308.
(69) Wu, G.; Neville, S. P.; Schalk, O.; Sekikawa, T.; Ashfold, M. N. R.; Worth, G. A.; Stolow, A. Excited State Non-Adiabatic Dynamics of N-Methylpyrrole: A Time-Resolved Photoelectron Spectroscopy and Quantum Dynamics Study. *J. Chem. Phys.* **2016**, *144*, 014309.
(70) Barbatti, M.; Lischka, H.; Salzmann, S.; Marian, C. M. UV Excitation and Radiationless Deactivation of Imidazole. *J. Chem. Phys.* **2009**, *130*, 034305.
(71) Devine, A. L.; Cronin, B.; Nix, M. G. D.; Ashfold, M. N. R. High Resolution Photofragment Translational Spectroscopy Studies of the Near Ultraviolet Photolysis of Imidazole. *J. Chem. Phys.* **2006**, *125*, 184302.
(72) Kuhlman, T. S.; Glover, W. J.; Mori, T.; Møller, K.B.; Martinez, T. J. Between Ethylene and Polyenes − the Non-Adiabatic Dynamics of Cis-Dienes. *Faraday Discuss.* **2012**, *157*, 193−212.
(73) Schalk, O.; Boguslavskiy, A. E.; Stolow, A. Substituent Effects on Dynamics at Conical Intersections: Cyclopentadienes. *J. Phys. Chem. A* **2010**, *114*, 4058−4064.
(74) Tao, H. L.; Levine, B. G.; Martinez, T. J. Ab Initio Multiple Spawning Dynamics Using Multi-State Second-Order Perturbation Theory. *J. Phys. Chem. A* **2009**, *113*, 13656−13662 and references therein..
(75) Pullen, S. H.; Anderson, N. A.; Walker, L. A.; Sension, R. J. The Ultrafast Photochemical Ring-Opening Reaction of 1,3-Cyclohexadiene in Cyclohexane. *J. Chem. Phys.* **1998**, *108*, 556−563.
(76) Garavelli, M.; Page, C. S.; Celani, P.; Olivucci, M.; Schmid, W. E.; Trushin, S. A.; Fuss, W. Reaction Path of a sub-200 fs Photochemical Electrocyclic Reaction. *J. Phys. Chem. A* **2001**, *105*, 4458−4469.
(77) Kosma, K.; Trushin, S. A.; Fuss, W.; Schmid, W. E. Cyclohexadiene Ring Opening Observed with 13 fs Resolution: Coherent Oscillations Confirm the Reaction Path. *Phys. Chem. Chem. Phys.* **2009**, *11*, 172−181.
(78) Arruda, B. C.; Sension, R. J. Ultrafast Polyene Dynamics: The Ring Opening of 1,3-Cyclohexadiene Derivatives. *Phys. Chem. Chem. Phys.* **2014**, *16*, 4439−4455.
(79) Adachi, S.; Sato, M.; Suzuki, T. Direct Observation of Ground-State Product Formation in a 1,3-Cyclohexadiene Ring-Opening Reaction. *J. Phys. Chem. Lett.* **2015**, *6*, 343−346.
(80) Pemberton, C. C.; Zhang, Y.; Saita, K.; Kirrander, A.; Weber, P. M. From the (1B) Spectroscopic State to the Photochemical Product of the Ultrafast Ring-Opening of 1,3-Cyclohexadiene: A Spectral Observation of the Complete Reaction Path. *J. Phys. Chem. A* **2015**, *119*, 8832−8845.
(81) Minitti, M. P.; Budarz, J. M.; Kirrander, A.; Robinson, J. S.; Ratner, D.; Lane, T. J.; Zhu, D.; Glownia, J. M.; Kozina, M.; Lemke, H. T.; et al. Imaging Molecular Motion: Femtosecond X-Ray Scattering of an Electrocyclic Chemical Reaction. *Phys. Rev. Lett.* **2015**, *114*, 255501.
(82) Schalk, O.; Geng, T.; Thompson, T.; Baluyot, N.; Thomas, R. D.; Tapavicza, E.; Hansson, T. Cyclohexadiene Revisited: A Time-Resolved Photoelectron Spectroscopy and Ab Initio Study. *J. Phys. Chem. A* **2016**, *120*, 2320−2329.
(83) Attar, A. R.; Bhattacherjee, A.; Pemmaraju, C. D.; Schnorr, K.; Closser, K. D.; Prendergast, D.; Leone, S. R. Femtosecond X-Ray Spectroscopy of an Electrocyclic Ring-Opening Reaction. *Science* **2017**, *356*, 54−59.
(84) Christensen, L.; Nielsen, J. H.; Brandt, C. B.; Madsen, C. B.; Madsen, L. B.; Slater, C. S.; Lauer, A.; Brouard, M.; Johansson, M. P.; Shepperson, B.; et al. Dynamic Stark Control of Torsional Motion by a Pair of Laser Pulses. *Phys. Rev. Lett.* **2014**, *113*, 073005.
(85) Matsuda, A.; Fushitani, M.; Takahashi, E. J.; Hishikawa, A. Visualizing Hydrogen Atoms Migrating in Acetylene Dication by Time-Resolved Three-Body and Four-Body Coulomb Explosion Imaging. *Phys. Chem. Chem. Phys.* **2011**, *13*, 8697−8704.
(86) Ibrahim, H.; Wales, B.; Beaulieu, S.; Schmidt, B. E.; Thire, N.; Fowe, E. P.; Bisson, E.; Hebeisen, C. T.; Wanie, V.; Giquere, M.; et al. Tabletop Imaging of Structural Evolutions in Chemical Reactions Demonstrated for the Acetylene Cation. *Nat. Commun.* **2014**, *5*, 4422.
(87) Burger, C.; Kling, N. G.; Siemering, R.; Alnaser, A. S.; Bergues, B.; Azzeer, A. M.; Moshammer, R.; de Vivie-Riedle, R.; Kuebel, M.; Kling, M. F. Visualization of Bond Rearrangements in Acetylene Using Near Single-Cycle Laser Pulses. *Faraday Discuss.* **2016**, *194*, 495−508.
(88) Boll, R.; Erk, B.; Coffee, R.; Trippel, D.; Kierspel, T.; Bomme, C.; Bozek, J.; Burkett, M.; Carron, S.; Ferguson, K. R.; et al. Charge Transfer in Dissociating Iodomethane and Fluoromethane Molecules Ionized by Intense Femtosecond X-Ray Pulses. *Struct. Dyn.* **2016**, *3*, 043207.

DOI: 10.1021/acs.jpclett.7b01219
J. Phys. Chem. Lett. 2017, 8, 3440−3451